Research Square

Preprints are preliminary reports that have not undergone peer review.
They should not be considered conclusive, used to inform clinical practice,
or referenced by the media as validated information.

# Clinical investigation of VES001, a novel oral small molecule sortilin receptor inhibitor, for the treatment of frontotemporal dementia

**Mads Kjolby**

MADS@BIOKEMI.AU.DK

Vesper Bio https://orcid.org/0000-0002-1043-6137

**Louise Klem**

Vesper Bio

**Daniel Dumas**

Centre for Human Drug Research

**Imogen J Swift**

Vesper Bio

**Sofie L Frandsen**

Vesper Bio

**Ditte Nedergaard Mikkelsen**

Vesper Bio

**Laerke Fensbaek**

Vesper Bio

**Yalçin Yavuz**

Centre for Human Drug Research

**Okke Merton**

Centre for Human Drug Research

**Jesminne Castricum**

Centre for Human Drug Research

**Simone Prichardt**

Vesper Bio

**Graham M Wynne**

Vesper Bio

**Anders Riisager**

Vesper Bio

**Nina Schultz**

Vesper Bio

**Paul B Little**

Vesper Bio
**Ove Pedersen**
Vesper Bio
**Eva Thijssen**
Centre for Human Drug Research
**Anders Nykjaer**
Vesper Bio
**Philip Kremer**
Centre for Human Drug Research & Leiden University Medical Centre https://orcid.org/0000-0003-0483-841X

---

**Article**

**Keywords:**

**Posted Date:** March 31st, 2026

**DOI:** https://doi.org/10.21203/rs.3.rs-8405910/v1

**License:** This work is licensed under a Creative Commons Attribution 4.0 International License.
Read Full License

**Additional Declarations: Yes** there is potential Competing Interest. Anders Nykjaer, Paul Little, and Mads Kjolby hold patents. Anders Nykjaer and Mads Kjolby are shareholders of Vesper Bio.

---

**Version of Record:** A version of this preprint was published at Nature Communications on September 14th, 2026. See the published version at https://doi.org/10.1038/s41467-026-77638-2.

# Clinical investigation of VES001, a novel oral small molecule sortilin receptor inhibitor, for the treatment of frontotemporal dementia

Louise Klem[1]*, Daniel Dumas[2,3]*, Imogen J Swift[1], Sofie L Frandsen[1], Ditte Nedergaard Mikkelsen[1], Laerke Fensbaek[1], Yalçin Yavuz[2], Okke Merton[2], Jesminne Castricum[2], Simone Prichardt[1], Graham M Wynne[1], Anders Riisager[1], Nina Schultz[1], Paul B Little[1], Ove Pedersen[1], Eva Thijssen[2], Anders Nykjaer[1,4], Philip Kremer[2,3], Mads Kjolby[1]

1. Vesper Bio Aps, Hauser Plads 10 1127, Copenhagen, Denmark
2. Centre for Human Drug Research, Zernikedreef 8, 2333 CL Leiden, Netherlands
3. Leiden University Medical Center, LUMC, Leiden, The Netherlands
4. PROMEMO, Department of Biomedicine, Aarhus University, Høegh-Guldberg Gade 10, Bldg. 1115-1116, 8000 Aarhus, Denmark.

*Co-first author

Corresponding author: Mads Kjolby[1]

E-mail: mfk@vesperbio.com

# Abstract

*GRN* gene haploinsufficiency reduces progranulin and causes frontotemporal dementia (FTD-*GRN*). Restoring progranulin to physiological levels counteracts the molecular deficit underlying the disease. VES001 is an orally administered small molecule sortilin inhibitor that increases progranulin by blocking its interaction with sortilin without downregulating sortilin. In preclinical studies, VES001 bound selectively to sortilin, showed no effects on other tested targets, and elevated progranulin in plasma, cerebrospinal fluid (CSF), and hippocampal interstitial fluid. In a first-in-human phase 1A study, healthy subjects received single and multiple ascending oral doses of VES001 over 7 days. VES001 displayed dose-proportional pharmacokinetics, blood-brain barrier penetration and was safe and well tolerated. Single dosing increased plasma progranulin, and repeated administration produced greater and more sustained PGRN increases in plasma and CSF. These findings establish pharmacological proof of mechanism for orally delivered sortilin inhibition and support further development of VES001 as a potential disease-modifying therapy for FTD-*GRN*. ClinicalTrials.gov identifier: NCT06226064

# Introduction

Frontotemporal dementia (FTD) is a progressive neurodegenerative disease marked by atrophy of the frontal and temporal lobes and is the second most common cause of early-onset dementia in individuals under 65 years (1). Epidemiological studies from Europe indicate that FTD accounts for 5–10% of all dementia cases, 10–20% of those with onset before 65 years, and affects 28 per 100,000 individuals aged 60–70-years (2, 3). Clinically, FTD manifests as progressive behavioral and/or language dysfunction, profoundly impairing quality of life (1, 3). Current treatments provide only symptomatic relief and do not target the underlying molecular pathology, underscoring an urgent need for disease-modifying therapies.

A strong genetic component underlies FTD, with 20–50% of FTD cases being familial (3, 4). Approximately 60% of these linked to mutations in 3 genes: chromosome 9 open reading frame 72, microtubule-associated protein tau, and the progranulin (PGRN) encoding gene (*GRN*) (3, 4). *GRN* loss-of-function mutations are found in 5–20% of familial FTD cases and 1–5% of sporadic FTD cases (5). These heterozygous mutations result in an approximately 50% reduction in PGRN levels and lead to development of FTD with complete penetrance (FTD-*GRN*) (2, 5). Therapeutic strategies that restore PGRN to physiological levels are therefore considered a rational and potentially disease-modifying approach for FTD-*GRN* (6-9).

PGRN elevation consistently suppresses inflammation and attenuates neurodegeneration across both PGRN-deficient and non-PGRN-deficient models (5, 10-21). PGRN interacts with several binding partners, including sortilin, a type I transmembrane receptor in neurons, and prosaposin with its receptors (22). Sortilin mediates endocytosis and lysosomal degradation of PGRN, acting as a major clearance receptor, while PGRN also enters lysosomes through interactions with prosaposin and low-density lipoprotein receptor-related protein 1 (LRP1) (22). Sortilin inhibition increases PGRN levels, and research shows that the anti-inflammation and neurotrophic effects of PGRN are independent of sortilin (20, 23-26). Importantly, sortilin itself also exerts pro-inflammatory effects and facilitates apoptosis through the cell surface complex with the P75 neurotrophin receptor ($P75^{NTR}$) (27-31).

Different strategies are being developed to elevate PGRN levels *in vivo*, including sortilin inhibition, delivery of modified or recombinant PGRN, and gene therapies designed to enhance *GRN* expression. Among these, sortilin inhibition using a small molecule in the neurotensin binding pocket (NTIS1) represents a particularly compelling approach. It may both restore PGRN levels and directly counteract sortilin-mediated inflammatory and apoptotic signaling, without

interfering with other important functions of sortilin, such as Trk receptor transport (32). This contrasts with other sortilin-targeting strategies, as an antibody (latozinemab) is known to downregulate sortilin and may impact functions of the receptor (32, 33).

Here, we report on the pre-clinical development of VES001 and the subsequent first-in-human single and multiple ascending dose studies in healthy volunteers, describing pharmacokinetics (PK) and the pharmacodynamic (PD) changes in PGRN levels. VES001 is an orally delivered small molecule, that inhibits the protein-protein interaction between sortilin and PGRN without impacting sortilin levels and with limited impact on other functions. Importantly it is also effective at crossing the blood-brain barrier, resulting in a favorable CNS exposure profile. Preclinical development experiments included evaluating *in vitro* binding to sortilin and other members of the receptor family (30), and an *in vitro* sortilin internalization/downregulation assay. Further preclinical evaluation included a rat microdialysis experiment, assessing PK/PD in plasma, cerebrospinal fluid (CSF), and hippocampal interstitial fluid (Hpc ISF). These preclinical studies led to the phase 1A clinical trial, designed to assess safety, tolerability, PK, and PD of both single and multiple ascending dose administrations in healthy volunteers.

# Results

## Pre-clinical evaluation of VES001

### VES001 selectively inhibits human sortilin without receptor downregulation *in vitro*

Grating-coupled interferometry analyses confirmed that VES001 binds human sortilin with high affinity (mean ± standard deviation (s.d.), $K_{on}$ = $1.55*10^6$ ± $4.88*10^5$ $M^{-1}s^{-1}$; $K_{off}$ = $8.35*10^{-2}$ ± $2.13*10^{-2}$ $s^{-1}$; $K_D$ = 55.1 ± 4.98 nM). No measurable binding to other members of the Vps10p family was detected (**Extended Data Figure 1**) (30).

Furthermore, VES001 showed no relevant inhibition or stimulation across a SafetyScreen 87 pharmacology panel and a panel of 8 cytochrome P450 enzymes.

In flow-cytometry assays, VES001 potently inhibited the interaction between human PGRN and sortilin in a HEK293-FL cell line, with an $IC_{50}$ (mean ± s.d.) of 4.424 ± 4.498 µM and a $K_i$ of 2.121 ± 2.106 µM. The mean and s.d. for the unbound fraction in human plasma was 10.3 ± 0.6% (recovery mean 92.3%). Notably, the tested concentrations of VES001 (3–9000 ng $mL^{-1}$) had no detectable effect on cell-surface or total sortilin protein levels in COLO792 cells, whereas a

latozinemab biosimilar reduced both by 50–60% (n = 6) (**Fig. 1a, b**). These findings demonstrate that VES001 acts through functional competitive inhibition rather than receptor down-regulation.

### VES001 penetrates the BBB and elevates PGRN *in vivo*

Following repeated oral administration in rats (n=7), VES001 was detected in Hpc ISF, CSF, and plasma with stable PK profiles (**Fig. 1c, d**). Peak mean concentrations were 815 ng $mL^{-1}$ at 2 h in Hpc ISF, 2175 ng $mL^{-1}$ at 4 h in CSF, and 29571 ng $mL^{-1}$ at 4 h in plasma, with Hpc ISF and CSF levels approximately 10-fold lower than plasma, when not adjusting for protein binding.

VES001 produced clear, time-dependent increases in PGRN in all compartments, separating from baseline by 1 h (plasma), 3 h (CSF), and 5 h (Hpc ISF) after the first dose (**Fig. 1e, f**). Maximal mean responses occurred at 9 h in Hpc ISF (6.12 ng $mL^{-1}$; 144% increase; 2.44-fold), 7 h in CSF (23.91 ng $mL^{-1}$; 93% increase; 1.93-fold), and 10 h in plasma (981.67 ng $mL^{-1}$; 114% increase; 2.14-fold). Vehicle-treated rats showed no significant change (n = 5). These data confirm BBB penetration and dose-dependent elevation of PGRN following systemic VES001 administration in a pre-clinical model.

## First-in-human evaluation in healthy volunteers

### Participant disposition and baseline characteristics

A total of 48 healthy adults were enrolled in the single-ascending-dose (SAD) study and completed dosing and follow-up (**Fig. 2a**). In the multiple-ascending-dose (MAD) study, 31 participants completed dosing and follow-up (**Fig. 2b**). One participant in MAD cohort 2 (2x180 mg) discontinued PK sampling for personal reasons unrelated to study conduct and was replaced. Baseline demographics were comparable across cohorts (**Table 1**).

### Safety and tolerability

VES001 was safe and well tolerated in healthy volunteers, with no deaths, serious adverse events, or discontinuations due to treatment-emergent adverse events. Adverse events were reported in 51.9% of SAD and 80.6% of MAD participants, most commonly mild headache and fatigue (**Extended Data Tables 1 and 4**). In the SAD study, most events were unrelated to treatment (23/28 events); in the MAD study, approximately 1/3 were unrelated (27/93 events). The incidence of headache (VES001: 22.2–62.5% vs placebo 16.7%) and fatigue (VES001: 22.2–50.0% vs placebo 16.7%) showed no dose-related trend. Clinical laboratory values, electrocardiograms (ECGs), and vital signs revealed no clinically meaningful differences between

VES001 and placebo. These findings indicate a favorable safety profile across the tested dose range.

# Single-ascending-dose (SAD) study

## Pharmacokinetics

Single oral doses of VES001 (10–990 mg) produced dose-proportional increases in plasma exposure (**Fig. 3a; Extended Data Table 2**). The mean terminal half-life ranged from 7.2 to 9.5 h for doses ≥ 30 mg, and individual concentration-time curves showed a biphasic decline (**Extended Data Fig. 2**). Under fed conditions, the median $T_{max}$ was 4 h compared with 1.5 h in the fasted state, whereas the overall exposure (AUC) was unchanged (**Fig. 3b**). VES001 was measurable in CSF 7 h post-dose in the 810 and 990 mg cohorts, yielding mean ± s.d. CSF/plasma ratios of 0.17 ± 0.05 and 0.16 ± 0.03, respectively (**Fig. 3e**). These data indicate dose-linear pharmacokinetics and blood–brain barrier penetration following single-dose administration.

## Pharmacodynamics

Single oral doses of VES001 produced dose-dependent but variable increases in plasma PGRN concentrations (**Fig. 3c, d; Extended Data Table 3**). No significant differences from placebo were observed at doses up to 270 mg, whereas the 810 mg and 990 mg cohorts exhibited statistically significant elevations relative to baseline and placebo (810 mg: 19.5% [95% CI 5.6–35.4%], $p < 0.01$; 990 mg: 18.8% [95% CI 4.4–35.2%], $p = 0.010$). Increases relative to baseline were evident within the first dosing day and persisted over 48 h, with peaks obtained at 48 h for 810 mg (35%) and at 24 h for 990 mg (27%). Mixed-model analysis identified main effects of baseline, treatment, and time (all $p < 0.0001$–$0.01$) with a significant treatment × time interaction ($p < 0.0001$), consistent with dose- and time-dependent modulation of PGRN.

CSF PGRN concentrations showed no significant differences between VES001 and placebo in the 810 mg and 990 mg cohorts (**Fig. 3f, g**). In this compartment, baseline levels were the only significant predictor of post-dose concentrations ($p < 0.0001$). These data suggest that single dosing increases plasma PGRN at higher doses but is insufficient to drive robust CSF changes, indicating that multiple dosing are required for stronger, more durable pharmacodynamic effects.

# Multiple-ascending-dose (MAD) study

## Pharmacokinetics

Repeated oral dosing for 7 days with VES001 (1×180 mg, 2×180 mg, or 2×450 mg) produced predictable, dose-proportional plasma pharmacokinetics (**Fig. 4a; Extended Data Table 5**). Mean steady-state concentrations were achieved by Day 3 for the 1×180 mg cohort and by Day 2 for the 2×180 mg and 2×450 mg cohorts, with accumulation ratios of 1.0, 1.26, and 1.19, respectively, consistent with minimal accumulation. The concentration-time profiles had similar shapes on Days 1 and 7 across regimens (**Fig. 5a**).

At 150 h after the first dose, mean ± s.d. CSF/plasma ratios were 0.11 ± 0.06, 0.19 ± 0.05, and 0.17 ± 0.09 for the 1×180, 2×180, and 2×450 regimens, respectively (**Fig. 4d**). Semi-quantitative profiling identified 13 plasma and 15 urinary metabolites; together, the metabolites accounted for < 6.6% of total drug-related exposure (**Extended Data Table 6**). Together, these findings confirm dose-proportional exposure, CNS penetration, and limited metabolite formation with repeated dosing.

## Pharmacodynamics

Consistent with the expectation from the SAD study, repeated twice-daily dosing of VES001 induced sustained, dose-dependent increases in PGRN in both plasma and CSF (**Fig. 4b, c, e, f; Extended Data Table 6**).

In plasma, PGRN was significantly elevated in the 2×180 mg and 2×450 mg cohorts relative to placebo (2×180 mg: 30.2% [95% CI 15.9–46.2%], $p < 0.0001$; 2×450 mg: 29.9% [95% CI 16.4–45.0%], $p < 0.0001$), whereas the 1×180 mg regimen produced no significant change. Mixed-model analysis confirmed main effects of baseline, treatment, and time, and a significant treatment × time interaction (all $p < 0.0001$), indicating a consistent pharmacodynamic effect across repeated dosing. Plasma PGRN concentrations in the 2×180 mg and 2×450 mg cohorts increased early during the first dosing day (starting 6 h post-dose) and continued to rise with repeated administration, remaining elevated for up to 48 h after the final dosing day (Day 7). The highest percentage increases were reached by Day 7 (2x180 mg: 25% ; 2x450 mg: 49%), indicating that pharmacodynamic effects may not yet have reached steady state (**Fig. 4c, d; Extended Data Table 6**).

In CSF, PGRN concentrations rose significantly in the 2×180 mg and 2×450 mg cohorts compared with placebo (2×180 mg: 17.2% [95% CI 7.0–28.5%], $p < 0.01$ ; 2×450 mg: 17.7% [95% CI 7.4–29.0%], $p < 0.01$), whereas the 1×180 mg regimen showed no significant effect. The magnitude

and persistence of these CSF effects (2x180 mg: 15% ; 2x450 mg; 18%) exceeded those seen in the SAD study, demonstrating that multiple dosing is required for a more substantial pharmacodynamic response (**Fig. 4.e, f; Extended Data Table 6**).

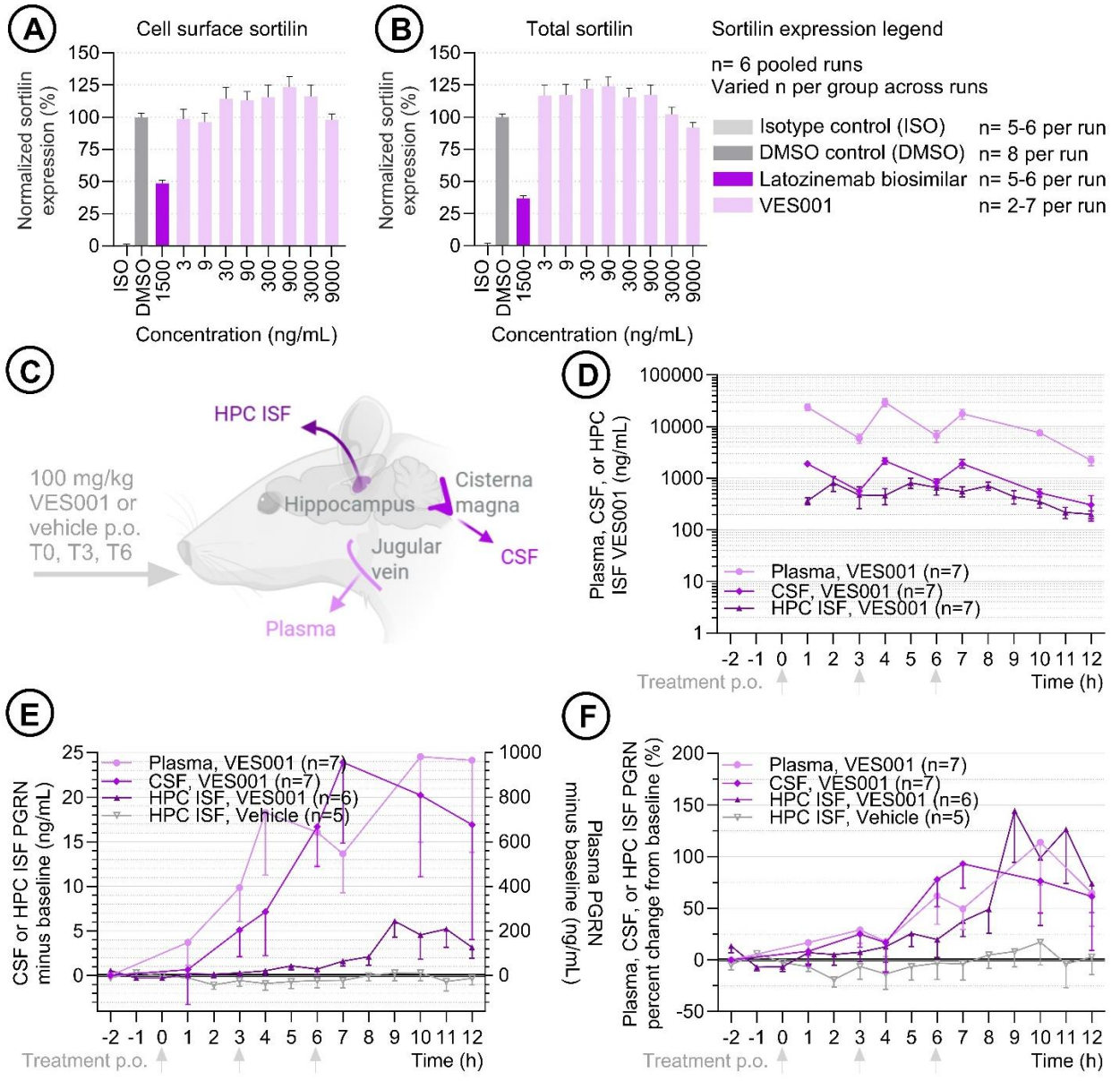



**Figure 1** | **Overview of VES001 pre-clinical data**. A–B) Results from the flowcytometry sortilin downregulation assay detecting changes in cell surface (A) and total (B) sortilin protein levels, comparing to a sortilin-targeting antibody (latozinemab biosimilar). C–F) Results from a rat microdialysis PK/PD experiment. C) Overview of the treatment and sampling. D) Plasma, CSF and HPC ISF compound levels (ng/mL). E) Absolute changes in PGRN from baseline (set to 0%) in CSF and HPC ISF og the left Y-axis and in plasma on the right Y-axis. F) Percentage changes in plasma, CSF, and HPC ISF PGRN from baseline (set to 0%). All data is reported as the mean and standard errors of the mean (SEM). n is listed directly in each graph.

**Table 1** | **Demography of phase 1A participants**

| | SAD cohort (n = 48) | MAD cohort (n = 31) |
|---|---|---|
| **Sex, n (%)** | | |
| Female | 18 (37.5%) | 11 (35.5%) |
| Male | 30 (62.5%) | 20 (64.5%) |
| **Race, n (%)** | | |
| Black or African American | 0 (0%) | 1 (3.2%) |
| Mixed | 2 (4.2%) | 1 (3.2) |
| White | 46 (95.8%) | 29 (93.5%) |
| **Age, years** | | |
| Mean ± s.d. | 28.2 ± 9.9 | 28.2 ± 8.7 |
| Median | 24 | 25 |
| Min–Max | 19–54 | 19–50 |
| **BMI (kg $m^{-2}$)** | | |
| Mean ± s.d. | 23.3 ± 2.61 | 23.1 ± 2.78 |
| Median | 23.1 | 22.1 |
| Min–Max | 18.8–30.4 | 18.0–29.3 |

BMI = body mass index; MAD = multiple ascending dose; SAD = single ascending dose; s.d. = standard deviation

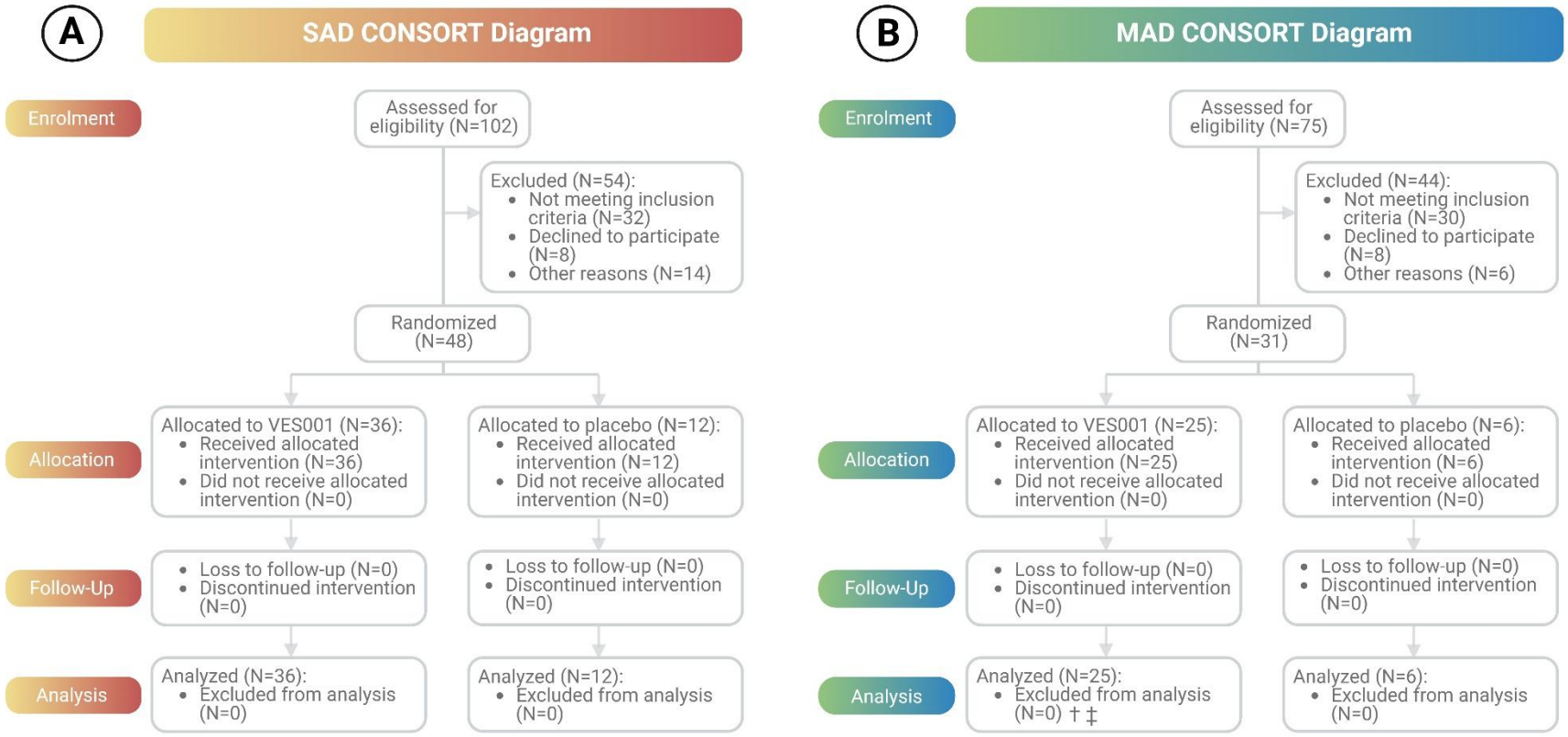



**Figure 2 | CONSORT diagrams of the single-ascending-dose (SAD) and multiple-ascending-dose (MAD) studies.** CONSORT diagrams showing participant flow through the SAD (A) and MAD (B) phases of the study. All participants completed dosing and safety follow-up. † In cohort 2, one participant missed one intermediate assessment day between the final dose and the last follow-up visit due to personal reasons unrelated to study conduct or VES001. Their PD and safety data (except for the missed assessments) were analyzed, but their PK data were unusable due to technical issues. This participant was replaced, resulting in 9 participants receiving VES001 in this cohort. ‡ In cohort 3, one participant declined the post-dose lumbar puncture; all other PK, PD, and safety assessments were performed and included in the analyses.

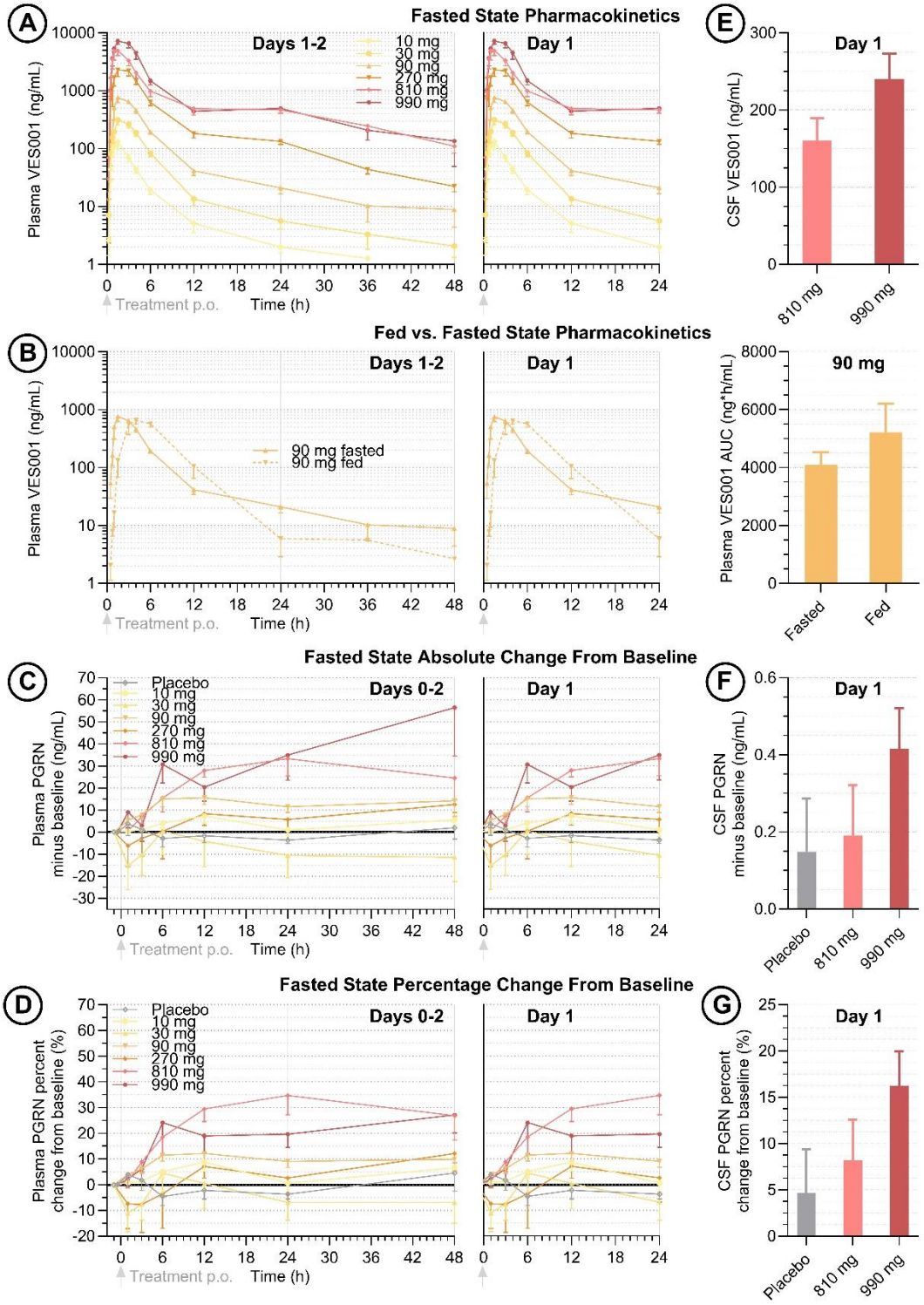



**Figure 3 | Ph1A VES001 SAD plasma and CSF PK/PD**. Plasma was sampled repeatedly throughout the experiment, while CSF was only sampled at –17 h (pre-dose) and at 7h (post-dose). A) Plasma compound levels (ng/mL) for the fasted cohorts. B) Plasma compound levels (ng/mL) and areas under the curve (AUC) (ng*h/mL) for the fed and fasted cohorts receiving 90 mg VES001. C) Absolute changes in plasma PGRN (ng/mL) for the fasted cohorts from the pre-dose baseline. D) Percentage change in plasma PGRN from the pre-dose baseline (set to 0%) for the fasted cohorts. E) Compound levels in CSF (ng/mL) for the fasted cohorts. F) Absolute change in CSF PGRN (ng/mL) from the pre-dose baseline for the fasted cohorts. G) Percentage change in CSF PGRN from baseline (set to 0%) for the fasted cohorts. The graphs depict the mean and the standard errors of the mean (SEM). n = 6 for each VES001 cohort, n = 12 for the plasma placebo cohort, and n = 4 for the CSF placebo cohort.

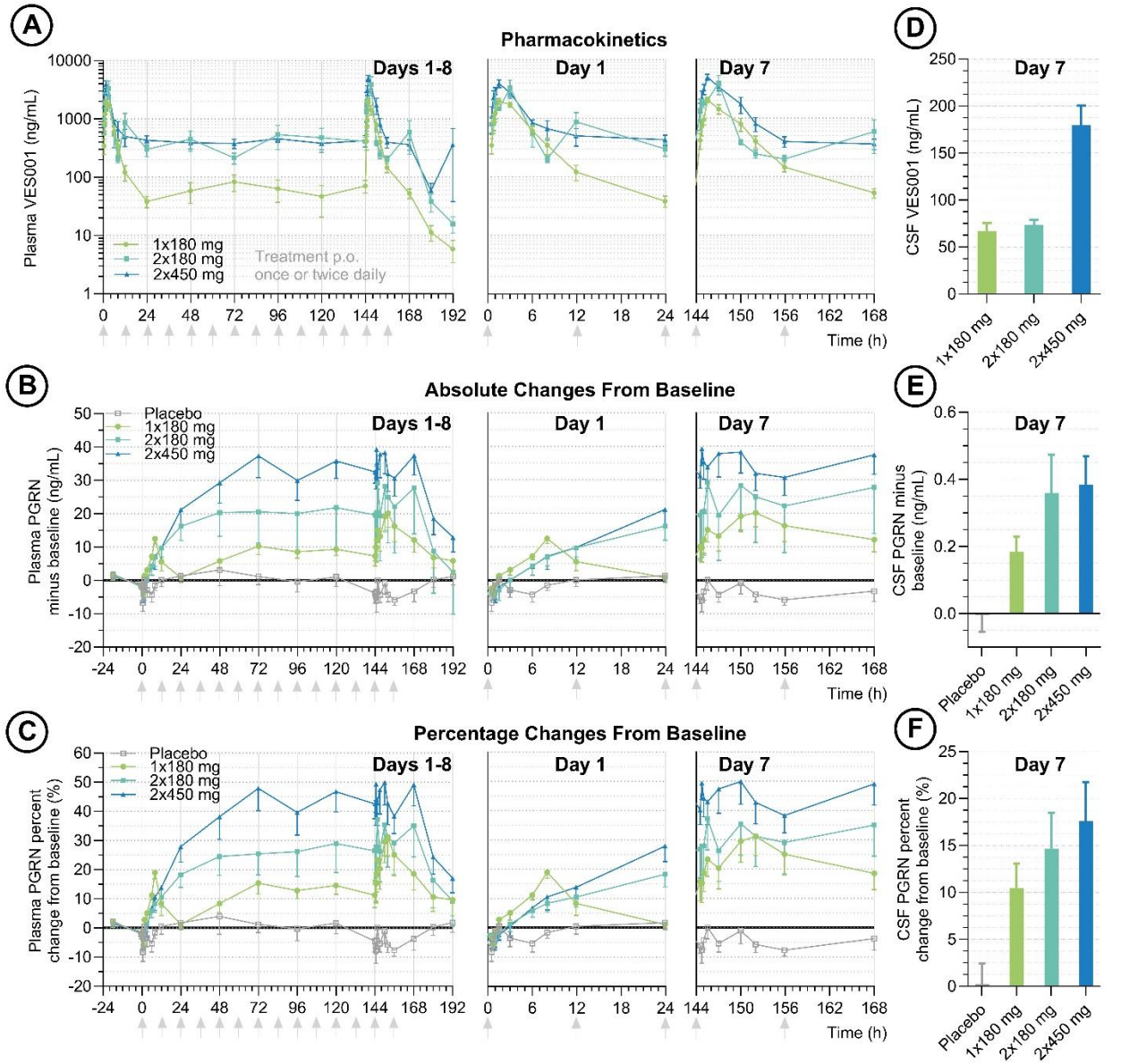



**Figure 4 | Ph1A VES001 MAD plasma and CSF PK/PD**. Plasma was sampled repeatedly throughout the experiment, while CSF was only sampled at –18 h (pre-dose) and at 150.2 h (post-dose). A) Plasma compound levels (ng/mL). B) Absolute changes in plasma PGRN (ng/mL) C) Percentage change in plasma PGRN from the pre-dose baseline (set to 0%). D) Compound levels in CSF (ng/mL). E) Absolute change in CSF PGRN (ng/mL) from the pre-dose baseline. F) Percentage change in CSF PGRN from the pre-dose baseline (set to 0%). The graphs depict the mean and the standard errors of the mean (SEM). In all graphs, the placebo cohort has n = 6 and the 1x180 mg cohort has n = 8. The 2x180 mg cohort has n = 8 for PK and n = 9 for PD. The 2x450 mg cohort has n = 8 for plasma, and n = 7 for CSF.

# Discussion

The rationale for PGRN normalization in FTD-*GRN* is supported by converging genetic and biomarker evidence. *Grn*-haploinsufficiency causes FTD-*GRN*, and reduced PGRN is directly linked to neuroinflammation and neurodegeneration (5, 14, 34). Drugs that reliably restore intra- and extracellular PGRN levels could therefore be a promising approach to disease modification.

This first-in-human study demonstrates that VES001, a novel and selective small molecule competitive inhibitor of sortilin, is safe and well tolerated in healthy adults and produces robust, dose-dependent increases in extracellular PGRN levels in plasma and CSF. These effects on PGRN levels are consistent with preclinical findings showing potent, specific binding of VES001 to human sortilin and inhibition of the PGRN-sortilin interaction. No non-specific activity was detected against other tested targets, which included a wide panel of targets and members of the Vps10p family (30). Notably, VES001 does not alter cell surface or total sortilin protein levels, while antibody-based approaches are known to cause receptor downregulation (33). Preclinical studies in wild-type cells and rodents — selected to match the physiology of healthy subjects — confirmed effective BBB penetration for the compound, resulting in downstream readouts confirming target engagement, including increased Hpc ISF PGRN concentrations measured by *in vivo* microdialysis. In the latter study, PGRN levels increased over time in all three compartments with steady levels of VES001. Together, these data provide a strong mechanistic foundation for targeting sortilin in FTD-*GRN*, a condition characterized by genetically driven PGRN deficiency.

In both the SAD and MAD studies, VES001 was well tolerated at all tested doses, with no serious adverse events or dose-limiting toxicities. The most common treatment-emergent adverse events (headache and fatigue) were mild and not dose-dependent.

In the SAD study, a dose-dependent increase in plasma PGRN was observed, although the magnitude of response varied across cohorts, possibly reflecting inter-individual differences in anthropometrics and smaller group sizes relative to the MAD study. Nevertheless, the findings in the SAD study suggest that repeated dosing would produce larger and more sustained PGRN elevations, a prediction confirmed in the MAD study.

In the MAD study, twice-daily administration caused greater and more sustained PGRN elevations in plasma and CSF than once-daily dosing. Interestingly, increases in PGRN levels continued to rise in magnitude even after PK had reached steady state. This temporal dissociation between

pharmacokinetics and pharmacodynamics suggests a delayed and progressive biological response, potentially mediated by saturation of buffering mechanisms such as prosaposin-PGRN complex formation (35, 36). The observation that PGRN continued to rise despite stable VES001 concentrations parallels preclinical findings, indicating that full pharmacodynamic expression may require sustained receptor inhibition.

Contextualization of these effects within the Genetic FTD Initiative (GENFI), which quantified PGRN using the same assay, provides a translational benchmark (37, 38). When superimposing the VES001-induced increases from the MAD study onto the reduced baseline levels observed in asymptomatic *GRN*-carriers, the projected concentrations approach those measured in non-carrier individuals. This supports the hypothesis that VES001 could normalize PGRN in genetically affected populations, a key therapeutic objective. Furthermore, previous studies of sortilin inhibition in *Grn*-haploinsufficient animals and asymptomatic human carriers have demonstrated amplified PGRN responses relative to controls, suggesting that patient populations may exhibit enhanced pharmacodynamic sensitivity (33).

Several limitations warrant consideration. The sample sizes, although sufficient for evaluating safety and pharmacology, limit the power to detect rarer adverse effects or subtle dose-response relationships. The 7-day treatment duration precludes conclusions about long-term safety or efficacy. In addition, differences in sortilin expression, baseline PGRN levels, or compensatory mechanisms between healthy volunteers and patients may influence the pharmacodynamic response. These aspects should be addressed in upcoming patient trials that combine extended dosing with patient-specific biomarker monitoring.

In conclusion, VES001 is a promising first-in-class therapeutic candidate for FTD-*GRN*. Its favorable safety profile, BBB penetration, and ability to elevate PGRN in humans, together with the mechanistic concordance between *in vitro*, *in vivo*, and clinical data provide a strong rationale for advancing to studies in genetically defined patient populations. Future trials will determine whether sustained PGRN normalization translates into disease modification.

# Methods

The following sections provide brief overviews of the methods and materials for supporting preclinical experiments, while the clinical trials are described in detail. The in-depth descriptions for preclinical experiments are available in the Supplementary Information.

## *In vitro* cell-based assays evaluating VES001

### Grating coupled interferometry (GCI):

***Sortilin:*** The direct *in vitro* binding properties of VES001 to recombinant human sortilin immobilized on a 4PCH chip were determined using Creoptix WAVEdelta equipment. The GCI assay involved three steps: 1) Chip conditioning and immobilization – the preparation of the 4PCH GCI chip prior to sortilin immobilization and the capturing of the progranulin upon the surface of a flow cell, 2) analyte screening – flowing VES001 over the immobilized sortilin upon the surface and a reference flow cell, and 3) data analysis. All measurements made were double referenced (blank and reference flow-cell subtracted). These steps were performed using the 'Kinetic Analysis' tool of the GCI 'WAVEcontrol' software with data fitted using a standard 1:1 kinetic BioModel. The software was used to calculate the association rate constant ($K_{on}$), dissociation rate constant ($K_{off}$), and the equilibrium dissociation constant ($K_D$) for each run, and the means and standard deviations (s.d.) were calculated across runs.

***Other Vps10p family members:*** The direct *in vitro* binding properties of VES001 to recombinant human SorCS1, SorCS2, SorCS3, and SorLA was conducted as done for sortilin.

### SafetyScreen87 panel and CYP panel:

The off-target binding properties of VES001 were tested in the commercially available Eurofins' SafetyScreen87 panel-FR at 10 µM *in vitro*. The target classes included G-protein-coupled receptors, ion channels, enzymes, and transporters. The full overview of the 87 targets is available on Eurofins website (39). Moreover, 10 µM VES001 was also analyzed with the commercially available Eurofins' Cytochrome P450 inhibition panel (overview available on Eurofins website) comprised of eight Cytochrome P450 isozymes (39). Compound binding was calculated as a percentage inhibition of the binding of a ligand specific for each target. Compound enzyme inhibition effect was calculated as the percentage inhibition of control enzyme activity. In vitro absorption was evaluated as the compound transporter inhibition effect, calculated as percentage inhibition of the vehicle control activity. Results showing an inhibition or stimulation higher than

50% would represent significant effects of the test compound. To assess *in vitro* metabolism, As previously, compound binding was calculated as a percentage inhibition of the binding of a ligand specific for each target and results showing an inhibition higher than 50% would represent significant effects of the test compound.

## Flowcytometry PGRN and sortilin assays:

VES001 $IC_{50}$ and $K_i$ values were determined in an *in vitro* flow cytometry displacement assay (MACSQuantX) using HEK293-FL cells. In brief, cells were harvested, counted (Luna II) and loaded onto a 384-well plate. VES001 and control compounds were then dispensed in duplicate as an 8-point concentration response curve (top concentration of 30 µM) and dimethyl sulfoxide (DMSO) normalized to 0.3%. Custom-made PGRN with a biotinylated Avi-tag was then prepared (120 nM) and 10 µL added to each well, followed by the addition of streptavidin-AF647 (10 µL). Using acquisition mode, median fluorescence intensity (MFI) values were collected and screening data analyzed using FlowJo software. $IC_{50}$ and $K_i$ values were then reported using a 4-parameter curve fit (variable slope model) and Cheng-Prussoff equation: $K_i = IC_{50} / [1 + (L/K_d)$.

## Sortilin Downregulation Assay by Flowcytometry:

The impact of VES001 on the cell surface and total sortilin protein levels was evaluated in an *in vitro* flowcytometry assay (MACSQuant X) using COLO792 cells. Permeabilized cells were used for the total sortilin levels, while non-permeabilized cells informed on the cell surface levels. Prior to permeabilization, the cells were treated for 24h with a wide concentration range of VES001 (3, 9, 30, 90, 300, 900, 3000, and 9000 ng/mL). VES001 was tested alongside a sortilin-targeting antibody known to downregulate sortilin (1500 ng/mL), as a positive control, DMSO, and a rabbit IgG isotype control. The experiment included 6 runs with varied n for each group within each run. Within each run, the data was normalized with the isotype control set to 0% and the DMSO control set to 100%. The normalized data was then pooled across runs and illustrated using GraphPad Prism (version 10.1.1).

## Rapid Equilibrium Dialysis (RED) on human plasma:

*In vitro* protein binding of VES001 in human plasma of mixed sex was determined using the Rapid Equilibrium Dialysis (RED) method and LC-MS/MS equipment. Technical triplets of VES001 and the positive control were incubated in plasma and then aliquots of donor side matrixes were collected and diluted with an equal volume of the blank receiver side matrix. All samples were protein precipitated by addition of a two-fold volume of internal standard solution. After

centrifugation, the supernatants were analyzed with LC/MS/MS to obtain the unbound fraction of test substance in plasma. The recovery sample was prepared by pooling the remaining amounts of spiked donor side matrixes (replicates) together and preparing these for analysis in the same manner as donor side samples. The sample was prepared for analysis immediately after starting the RED experiment. The unbound fraction and recovery were calculated from the analyte peak areas and the matrix volumes.

## *In vivo* microdialysis study on VES001 in rats

The microdialysis study was conducted in thirteen fasted male Sprague-Dawley rats, which were divided into two treatment groups to receive either vehicle or VES001. Stereotaxic surgery was used to position microdialysis probes. All rats were implanted with guides and push-pull microdialysis probes targeting the left hippocampus to measure PGRN concentrations. In animals assigned to receive VES001, guides and MetaQuant microdialysis probes were additionally placed in the right hippocampus to measure VES001 concentrations. These animals were also surgically equipped for cerebrospinal fluid (CSF) sampling from the cisterna magna and blood collection from the jugular vein. VES001 was formulated in 20% sulfobutylether-β-cyclodextrin in deionized water at a concentration of 20 mg/mL and administered by oral gavage at a dose of 100 mg/kg in a volume of 5 mL/kg. A total of 6 rats received the vehicle, and 7 rats were administered 100 mg/kg of VES001. All rats received oral doses at 0, 3, and 6 hours relative to the first administration. Food was withdrawn 2 hours before the first dose and returned 6 hours after the first dose. This pharmacokinetic (PK)/pharmacodynamic (PD) experiment commenced one day following surgery. Compound concentrations of VES001 were quantified using high-performance liquid chromatography coupled with tandem mass spectrometry (HPLC-MS/MS), with data adjusted for probe recovery. Quantification of rat PGRN was performed using a commercially available ELISA kit, following the manufacturer’s protocol. PGRN results were expressed as both the absolute and percentage changes from baseline. All compound and PGRN data were analyzed and visualized using GraphPad Prism (version 10.1.1).

# First-in-human phase 1 study

## Design

This single-center, randomized, double-blind, placebo-controlled first-in-human Phase 1 trial included single ascending dose (SAD) and multiple ascending dose (MAD) cohorts (EU CTR 2023-505847-38-00). The study was conducted at the Centre for Human Drug Research in Leiden, the Netherlands between 19 Oct 2023 and 26 Jul 2024.

The SAD part comprised 6 cohorts of healthy study participants receiving single doses of VES001 (10–990 mg) or placebo (6:2 ratio per cohort; pooled placebo N = 12) (**Fig. 5a**). Sentinel dosing was used for each cohort. Participants were admitted on Day –1, dosed in a fasted state on Day 1, remained in-house through Day 3, and returned for follow-up on Day 8 (±2 days) (**Fig. 5b**). Plasma PK and PGRN levels were sampled pre-dose and at designated post-dose time points on Days 1–3. CSF was collected via lumbar puncture pre-dose and at 7h post-dose in the placebo, 810 mg, and 990 mg VES001 cohorts (**Fig. 5c**). Cohort 3 completed a second visit after a washout period of at least 4 weeks to assess the effect of food, receiving the same dose in a fed state. A dose escalation review of the fasted visit of cohort 3 and safety review of at least 6 participants of cohort 4 up to at least 48 hours was conducted prior to the food effect visit.

The MAD study included 3 cohorts dosed with VES001 (180 mg once daily, 180 mg twice daily, or 450 mg twice daily) or placebo for 7 days (8:2 ratio; pooled placebo N = 6) (**Fig. 5a**). Participants were admitted on Day –1 and remained in-house through 48 hours post-final dose (Day 9), with follow-up on Day 15 (± 2 days) (**Fig. 5b**). Plasma PK and PGRN were measured on Days 1–9 and on Day 15. CSF samples were collected on Day –1 (baseline) and Day 7 (**Fig. 5c**).

Participants were screened within 42 days prior to dosing. Dose escalation decisions were based on safety, PK, and plasma PGRN data from previous cohorts, with PGRN evaluation lagging by no more than one cohort.

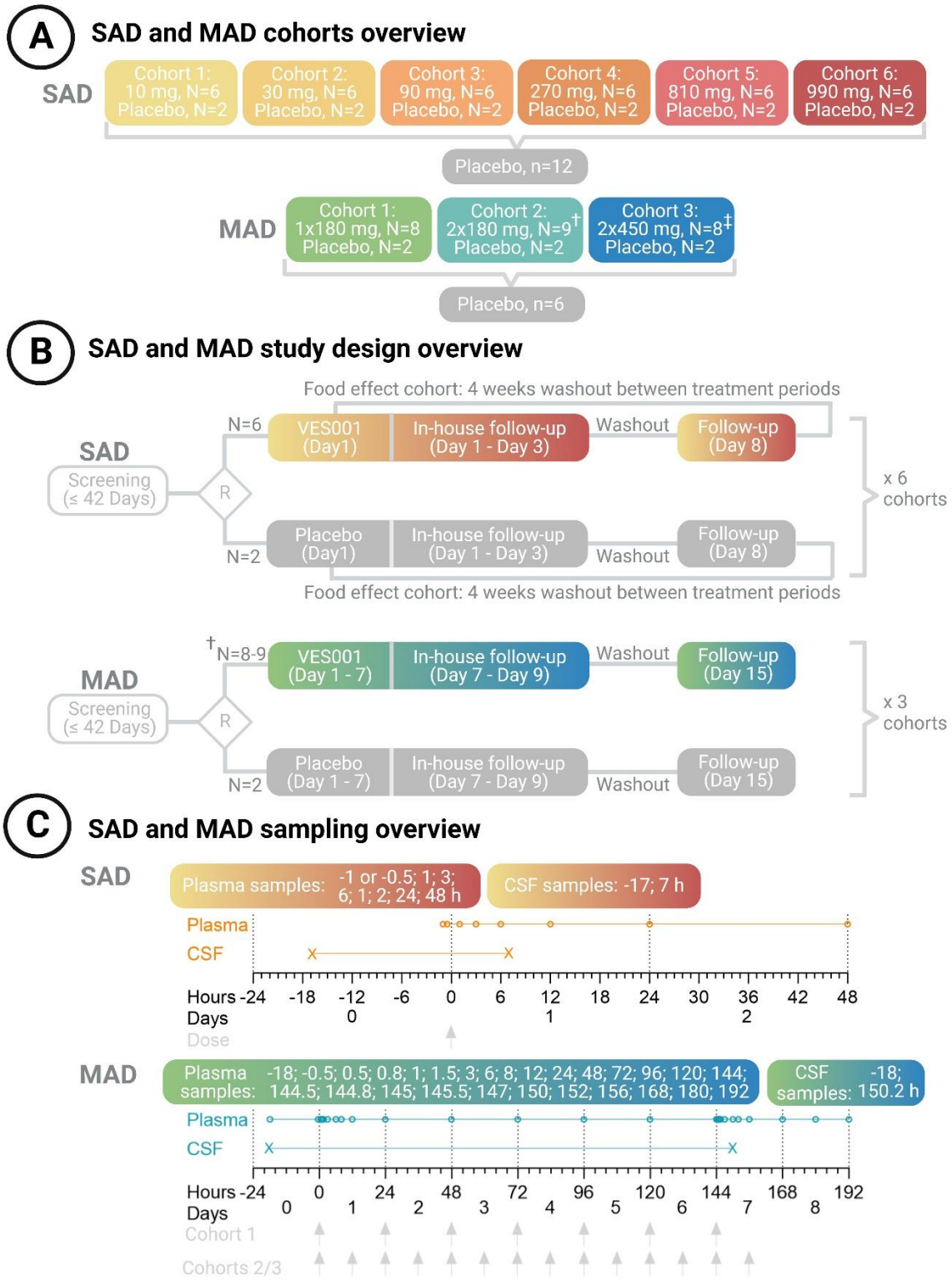



**Figure 5** | Schematic of Study design. MAD = multiple ascending dose; N = number of participants; R = Randomization; SAD = single ascending dose. † In cohort 2, one participant missed one intermediate assessment day between the final dose and the last follow-up visit due to personal reasons unrelated to study conduct or VES001. Their PD and safety data (except for the missed assessments) were analyzed, but their PK data were unusable due to technical issues. This participant was replaced, resulting in 9 participants

receiving VES001 in this cohort. ‡ In cohort 3, one participant declined the post-dose lumbar puncture; all other PK, PD, and safety assessments were performed and included in the analyses.

## Participants

Eligible participants were healthy adults aged 18–55 years with a BMI of 18–32 kg/m² and a minimum weight of 50 kg. Effective contraception was required during the study and for 90 days post-treatment.

Exclusion criteria included medical conditions or treatments potentially interfering with study assessments, such as neurological disorders, recent malignancy, significant head trauma, severe allergies, abnormal lab results, or infectious diseases (Hepatitis B/C, HIV). Heavy smokers or those unable to abstain were also excluded.

## IMP administration

VES001 was formulated as a pure solid compound without excipients in gelatin capsules (10, 30, 90, or 180 mg). Placebo capsules were visually identical. All study treatments were prepared at the Leiden University Medical Centre Pharmacy, The Netherlands.

Doses were administered orally with 300 mL of still water after a 10-hour fast, or, for the food-effect arm, following a high-fat meal. In twice daily regimens, the second dose was given 2 hours after fasting. The starting dose (10 mg) was 100-fold below the No Observed Adverse Event Level in dogs (30 mg/kg in dogs, which converts to 1,169 mg in a 70 kg human) and 10-fold below the Minimum Anticipated Biological Effect Level in rats (9.29 mg/kg in rats, which converts to 105.4 mg in human).

## Procedures

The primary objective was to assess the safety and tolerability of single and multiple doses of VES001. Safety endpoints included adverse events (AEs), serious unexpected suspected adverse reactions (SUSARs), changes in lab values, ECGs, vital signs, physical/neurological exams, and Columbia-Suicide Severity Rating Scale (C-SSRS) scores.

Secondary objectives assessed plasma and CSF PK following single, multiple, and food-effect dosing. PK parameters included $AUC_{0–inf}$, $AUC_{0–last}$ (SAD/food-effect only), % extrapolated AUC, $C_{max}$, $T_{max}$, $T_{lag}$, $T_{½}$, CL/F, $V_z$/F, and accumulation ratio (MAD only). CSF endpoints included plasma/CSF ratios in SAD cohorts 5–6 and MAD steady-state cohorts.

Exploratory objectives included measuring PGRN concentrations in plasma and CSF and semi-quantitative analysis of VES001 metabolites in plasma and urine.

## Human plasma and CSF progranulin analysis

PGRN concentration was quantified in plasma and CSF using a previously developed Meso Scale Discovery (MSD)-based immunoassay (38). In brief, blocking buffer (0.5% bovine serum albumin (BSA), in PBS-T (0.05% Tween-20 in 1X phosphate buffered saline)) was added to a streptavidin-coated MSD plate (MSD, L15SA-1) and incubated overnight at 2–8°C. The plate was then washed with PBS-T (a step conducted before the addition of each reagent), and biotinylated human PGRN capture antibody added (Biotechne R&D Systems, BAF2420, URL0321101) followed by a 1 h incubation at room temperature (RT). The standard curve (7.813–5000 pg/mL) was prepared using recombinant human PGRN (Biotechne R&D Systems, 2420-PG, MQW1021101) diluted in assay buffer (0.25% BSA in PBS-T). Standards and samples were then added to the plate and incubated for 2 h at RT. The detection antibody (Biotechne R&D Systems, MAB2420, WWO0220081) was added and incubated for 1 h at RT, followed by the addition of the secondary goat anti-mouse antibody with SULFO-TAG (MSD, R32AC-5, W0021235S) and a further 1 h incubation at RT. Finally, the electrochemical signal was generated by the addition of MSD read buffer GOLD (MSD, R92TG-2) and light emission read using a QuickPlex SQ120 plate reader (MSD, 13001801081059). Data was processed with MSD Discovery Workbench® 4.0.12 and SoftMax Pro GxP 7.0.3 with acceptance criteria reported in the appendix. Due to variability in baseline PGRN levels, the results were reported as the absolute changes in PGRN from baseline and the percentage change in PGRN from baseline and illustrated using GraphPad Prism (version 10.1.1).

## Human plasma and CSF compound analysis

VES001 was quantified in human plasma and CSF by an initial protein precipitation followed by LC-MS/MS analysis. In brief, VES001 and an internal standard analog (dexamethasone) were isolated from 20 µL CSF or plasma using protein precipitation. Calibration standards in the range from 1.00 to 5000 ng/mL used for method qualification were freshly prepared in human CSF or plasma on the day of analysis. Chromatographic separation was conducted using an Acquity UPLC column (Waters, HSS T3 1.8 µm 2.1 X 50 mm) with mobile phases of Buffer A: 0.1% formic acid (FA) in ultra-pure water (UPW) and Buffer B: 0.1% FA 84% acetonitrile (ACN), 0.1% FA. This U-HPLC was coupled to a QTRAP6500+ tandem mass spectrometer with ion spray in positive multiple reaction monitoring mode. QC samples were loaded regularly between runs and data

acquisition, peak area integration and regression performed using Analyst software (version 1.7.2) from AB Sciex. Concentrations were calculated using 13-point curves with weighted linear regression and illustrated using GraphPad Prism (version 10.1.1). Detailed LC-MS/MS methods and assay validation can be found in the Supplementary Information.

## Statistical analysis

All safety and statistical programming were conducted with SAS 9.4 for Windows or newer (SAS Institute, Inc.). PK non-compartmental analysis was conducted with R 3.6.1 for Windows or newer (R Foundation for Statistical Computing/R Development Core Team, Vienna, Austria, 2019). No imputation was performed for missing data. Multiplicity adjustments were not applied.

Participant disposition and demographic information was summarized for the treated population. Safety analyses were based on all enrolled participants who received at least one dose of study treatment.

Mean plasma and CSF concentrations of VES001 were calculated for each time point. The repeatedly measured pharmacodynamic endpoint of PGRN concentration in plasma was summarized by treatment group and time point using descriptive statistics, including sample size (n), mean, geometric mean, standard deviation (s.d.), standard error of the mean (s.e.m.), coefficient of variation (CV), geometric CV%, median, minimum, and maximum values. These data were further illustrated graphically as absolute and % change from baseline over time with s.d. represented by error bars. Similarly, single-measure pharmacodynamic endpoint of PGRN concentration in CSF, was summarized using the same descriptive statistics and presented graphically via box-and-whisker plots stratified by treatment and time. Specifically for the calculations of the CSF/plasma ratio, in part A this was calculated by dividing individual VES001 CSF sample concentrations, taken at 7h03m nominal time, by the individual VES001 plasma concentration, taken at 6h00m nominal time. In part B, the Plasma/CSF ratios were calculated to the plasma concentration at sampling time T, where the difference between the CSF sampling time and the plasma sampling time is minimal. In this case that meant that the plasma samples at 6 h after Dose 7 for Cohort 1 and after Dose 13 for Cohort 2 and 3 were used to calculate the plasma/CSF ratio. For the urine analysis, semiquantitative analysis was performed to assess how many metabolites were present and what their relative abundance was.

PD endpoints, including PGRN concentrations in plasma and CSF, were natural log-transformed prior to inferential analyses to stabilize variance and normalize distributions. Afterward, repeated PD measurements, such as plasma PGRN concentrations, were analyzed using a mixed-model

analysis of covariance (ANCOVA) with fixed effects for treatment, time, and their interaction, adjusting for the (averaged) baseline value as a covariate. Subject was included as a random effect to account for within-subject correlation. Single PD measurements, such as PGRN concentrations in CSF, were analyzed using a mixed-model analysis of variance (ANOVA) with similar fixed and random effects structures. Estimates derived from the models are on the log scale and were back-transformed to the original scale for reporting. These back-transformed estimates represent geometric means or ratios of geometric means, reflecting multiplicative treatment effects, thus treatment effects are interpreted as fold-changes relative to baseline.

## Ethical considerations

The study adhered to the protocol, ICH GCP, the Declaration of Helsinki, and local regulations (Dutch Medical Research in Human Subjects Act). Ethics approval was obtained prior to initiation, and written informed consent was provided by all participants prior to participating in the study.

# References


1. Miyagawa, T., Brushaber, D., Syrjanen, J., Kremers, W., Fields, J., Forsberg, L.K., Heuer, H.W., Knopman, D., Kornak, J., Boxer, A., et al. (2020). Utility of the global CDR((R)) plus NACC FTLD rating and development of scoring rules: Data from the ARTFL/LEFFTDS Consortium. Alzheimers Dement 16, 106-117. 10.1002/alz.12033.

2. Eriksen, J.L., and Mackenzie, I.R. (2008). Progranulin: normal function and role in neurodegeneration. J Neurochem 104, 287-297. 10.1111/j.1471-4159.2007.04968.x.

3. Kirshner, H. (2016). Frontotemporal Dementia and Frontotemporal Lobar Degeneration. emedicine.medscape.com/article/1135164.

4. Rojas, J.C., Wang, P., Staffaroni, A.M., Heller, C., Cobigo, Y., Wolf, A., Goh, S.-Y.M., Ljubenkov, P.A., Heuer, H.W., Fong, J.C., et al. (2021). Plasma neurofilament light for prediction of disease progression in familial frontotemporal lobar degeneration. Neurology 96, e2296-e2312. 10.1212/WNL.0000000000011848.

5. Amin, S., Carling, G., and Gan, L. (2022). New insights and therapeutic opportunities for progranulin-deficient frontotemporal dementia. Curr Opin Neurobiol 72, 131-139. 10.1016/j.conb.2021.10.001.

6. Baker, M., Mackenzie, I.R., Pickering-Brown, S.M., Gass, J., Rademakers, R., Lindholm, C., Snowden, J., Adamson, J., Sadovnick, A.D., Rollinson, S., et al. (2006). Mutations in progranulin cause tau-negative frontotemporal dementia linked to chromosome 17. Nature 442, 916-919. 10.1038/nature05016.

7. Carecchio, M., Fenoglio, C., Cortini, F., Comi, C., Benussi, L., Ghidoni, R., Borroni, B., De Riz, M., Serpente, M., Cantoni, C., et al. (2011). Cerebrospinal fluid biomarkers in Progranulin mutations carriers. J Alzheimers Dis 27, 781-790. 10.3233/JAD-2011-111046.

8. Cruts, M., and Van Broeckhoven, C. (2008). Loss of progranulin function in frontotemporal lobar degeneration. Trends Genet 24, 186-194. 10.1016/j.tig.2008.01.004.

9. Galimberti, D., Fenoglio, C., Cortini, F., Serpente, M., Venturelli, E., Villa, C., Clerici, F., Marcone, A., Benussi, L., Ghidoni, R., et al. (2010). GRN variability contributes to sporadic frontotemporal lobar degeneration. J Alzheimers Dis 19, 171-177. 10.3233/JAD-2010-1225.

10. Beel, S., Herdewyn, S., Fazal, R., De Decker, M., Moisse, M., Robberecht, W., Van Den Bosch, L., and Van Damme, P. (2018). Progranulin reduces insoluble TDP-43 levels, slows down axonal degeneration and prolongs survival in mutant TDP-43 mice. Mol Neurodegener 13, 55. 10.1186/s13024-018-0288-y.

11. Egashira, Y., Suzuki, Y., Azuma, Y., Takagi, T., Mishiro, K., Sugitani, S., Tsuruma, K., Shimazawa, M., Yoshimura, S., Kashimata, M., et al. (2013). The growth factor progranulin attenuates neuronal injury induced by cerebral ischemia-reperfusion through the suppression of neutrophil recruitment. J Neuroinflammation 10, 105. 10.1186/1742-2094-10-105.

12. Guan, Z., Chen, Z., Fu, S., Dai, L., and Shen, Y. (2020). Progranulin Administration Attenuates beta-Amyloid Deposition in the Hippocampus of 5xFAD Mice Through Modulating BACE1 Expression and Microglial Phagocytosis. Front Cell Neurosci 14, 260. 10.3389/fncel.2020.00260.

13. Laird, A.S., Van Hoecke, A., De Muynck, L., Timmers, M., Van den Bosch, L., Van Damme, P., and Robberecht, W. (2010). Progranulin is neurotrophic in vivo and protects against a mutant TDP-43 induced axonopathy. PLoS One 5, e13368. 10.1371/journal.pone.0013368.

14. Martens, L.H., Zhang, J., Barmada, S.J., Zhou, P., Kamiya, S., Sun, B., Min, S.-W., Gan, L., Finkbeiner, S., Huang, E.J., and Farese, R.V. (2012). Progranulin deficiency promotes neuroinflammation and neuron loss following toxin-induced injury. The Journal of Clinical Investigation 122, 3955-3959. 10.1172/JCI63113.

15. Pickford, F., Marcus, J., Camargo, L.M., Xiao, Q., Graham, D., Mo, J.R., Burkhardt, M., Kulkarni, V., Crispino, J., Hering, H., and Hutton, M. (2011). Progranulin is a chemoattractant for microglia and stimulates their endocytic activity. Am J Pathol 178, 284-295. 10.1016/j.ajpath.2010.11.002.

16. Tang, W., Lu, Y., Tian, Q.-Y., Zhang, Y., Guo, F.-J., Liu, G.-Y., Syed, N.M., Lai, Y., Lin, E.A., Kong, L., et al. (2011). The growth factor progranulin binds to TNF receptors and is therapeutic against inflammatory arthritis in mice. Science 332, 478-484. 10.1126/science.1199214.

17. Tao, J., Ji, F., Wang, F., Liu, B., and Zhu, Y. (2012). Neuroprotective effects of progranulin in ischemic mice. Brain Res 1436, 130-136. 10.1016/j.brainres.2011.11.063.

18. Van Kampen, J.M., Baranowski, D., and Kay, D.G. (2014). Progranulin gene delivery protects dopaminergic neurons in a mouse model of Parkinson's disease. PLoS One 9, e97032. 10.1371/journal.pone.0097032.

19. Van Kampen, J.M., and Kay, D.G. (2017). Progranulin gene delivery reduces plaque burden and synaptic atrophy in a mouse model of Alzheimer's disease. PLoS One 12, e0182896. 10.1371/journal.pone.0182896.

20. Xu, J., Xilouri, M., Bruban, J., Shioi, J., Shao, Z., Papazoglou, I., Vekrellis, K., and Robakis, N.K. (2011). Extracellular progranulin protects cortical neurons from toxic insults by activating survival signaling. Neurobiol Aging 32, 2326 e2325-2316. 10.1016/j.neurobiolaging.2011.06.017.

21. Yin, F., Banerjee, R., Thomas, B., Zhou, P., Qian, L., Jia, T., Ma, X., Ma, Y., Iadecola, C., Beal, M.F., et al. (2010). Exaggerated inflammation, impaired host defense, and neuropathology in progranulin-deficient mice. J Exp Med 207, 117-128. 10.1084/jem.20091568.

22. Zhou, X., Sun, L., Bastos de Oliveira, F., Qi, X., Brown, W.J., Smolka, M.B., Sun, Y., and Hu, F. (2015). Prosaposin facilitates sortilin-independent lysosomal trafficking of progranulin. J Cell Biol 210, 991-1002. 10.1083/jcb.201502029.

23. Ding, H., Wei, J., Zhao, Y., Liu, Y., Liu, L., and Cheng, L. (2017). Progranulin derived engineered protein Atsttrin suppresses TNF-alpha-mediated inflammation in intervertebral disc degenerative disease. Oncotarget 8, 109692-109702. 10.18632/oncotarget.22766.

24. Gass, J., Lee, W.C., Cook, C., Finch, N., Stetler, C., Jansen-West, K., Lewis, J., Link, C.D., Rademakers, R., Nykjaer, A., and Petrucelli, L. (2012). Progranulin regulates neuronal outgrowth independent of sortilin. Mol Neurodegener 7, 33. 10.1186/1750-1326-7-33.

25. Nguyen, A.D., Nguyen, T.A., Zhang, J., Devireddy, S., Zhou, P., Karydas, A.M., Xu, X., Miller, B.L., Rigo, F., Ferguson, S.M., et al. (2018). Murine knockin model for progranulin-deficient frontotemporal dementia with nonsense-mediated mRNA decay. Proc Natl Acad Sci U S A 115, E2849-E2858. 10.1073/pnas.1722344115.

26. Wang, B.C., Liu, H., Talwar, A., and Jian, J. (2015). New discovery rarely runs smooth: an update on progranulin/TNFR interactions. Protein Cell 6, 792-803. 10.1007/s13238-015-0213-x.

27. Jakobsen, T.S., Ostergaard, J.A., Kjolby, M., Birch, E.L., Bek, T., Nykjaer, A., Corydon, T.J., and Askou, A.L. (2023). Sortilin Inhibition Protects Neurons From Degeneration in the Diabetic Retina. Invest Ophthalmol Vis Sci 64, 8. 10.1167/iovs.64.7.8.

28. Nykjaer, A., Lee, R., Teng, K.K., Jansen, P., Madsen, P., Nielsen, M.S., Jacobsen, C., Kliemannel, M., Schwarz, E., Willnow, T.E., et al. (2004). Sortilin is essential for proNGF-induced neuronal cell death. Nature 427, 843-848. 10.1038/nature02319.

29. Nykjaer, A., and Willnow, T.E. (2012). Sortilin: a receptor to regulate neuronal viability and function. Trends Neurosci 35, 261-270. 10.1016/j.tins.2012.01.003.

30. Salasova, A., Monti, G., Andersen, O.M., and Nykjaer, A. (2022). Finding memo: versatile interactions of the VPS10p-Domain receptors in Alzheimer's disease. Mol Neurodegener 17, 74. 10.1186/s13024-022-00576-2.

31. Jansen, P., Giehl, K., Nyengaard, J.R., Teng, K., Lioubinski, O., Sjoegaard, S.S., Breiderhoff, T., Gotthardt, M., Lin, F., Eilers, A., et al. (2007). Roles for the pro-neurotrophin receptor sortilin in neuronal development, aging and brain injury. Nat Neurosci 10, 1449-1457. 10.1038/nn2000.

32. Vaegter, C.B., Jansen, P., Fjorback, A.W., Glerup, S., Skeldal, S., Kjolby, M., Richner, M., Erdmann, B., Nyengaard, J.R., Tessarollo, L., et al. (2011). Sortilin associates with Trk receptors to enhance anterograde transport and neurotrophin signaling. Nat Neurosci 14, 54-61. 10.1038/nn.2689.

33. Kurnellas, M., Mitra, A., Schwabe, T., Paul, R., Arrant, A.E., Roberson, E.D., Ward, M., Yeh, F., Long, H., and Rosenthal, A. (2023). Latozinemab, a novel progranulin-elevating therapy for frontotemporal dementia. J Transl Med 21, 387. 10.1186/s12967-023-04251-y.

34. Ghidoni, R., Benussi, L., Glionna, M., Franzoni, M., and Binetti, G. (2008). Low plasma progranulin levels predict progranulin mutations in frontotemporal lobar degeneration. Neurology 71, 1235-1239. 10.1212/01.wnl.0000325058.10218.fc.

35. Nicholson, A.M., Finch, N.A., Almeida, M., Perkerson, R.B., van Blitterswijk, M., Wojtas, A., Cenik, B., Rotondo, S., Inskeep, V., Almasy, L., et al. (2016). Prosaposin is a regulator of progranulin levels and oligomerization. Nature Communications 7, 11992. 10.1038/ncomms11992.

36. Zhou, X., Sullivan, P.M., Sun, L., and Hu, F. (2017). The interaction between progranulin and prosaposin is mediated by granulins and the linker region between saposin B and C. J Neurochem 143, 236-243. 10.1111/jnc.14110.

37. Swift, I. (2024). Developing novel fluid biomarkers for progranulin-associated frontotemporal dementia. PhD (University College London).

38. Suárez-Calvet, M., Capell, A., Araque Caballero, M.Á., Morenas-Rodríguez, E., Fellerer, K., Franzmeier, N., Kleinberger, G., Eren, E., Deming, Y., Piccio, L., et al. (2018). CSF progranulin increases in the course of Alzheimer's disease and is associated with sTREM2, neurodegeneration and cognitive decline. EMBO Mol Med 10. 10.15252/emmm.201809712.

39. EurofinsDiscovery. SafetyScreen87 Panel - FR. https://emea.eurofinsdiscovery.com/catalog/safetyscreen87-panel-fr/P342.

## Acknowledgements

The team would like to thank Manuel Javier Cases-Thomas, who had a critical role in the design, selection, and early characterization of VES001. The preclinical work to characterize VES001 was conducted in collaboration with the following contract research organizations: DomaineX LTD, Charles River Laboratories, Symeres, Sygnature Discovery, Anapharm, and Ardena. PROMEMO is supported by the Danish National Research Foundation (grant no DNRF133).

## Supplementary Files

This is a list of supplementary files associated with this preprint. Click to download.

- Supplementarymaterial.docx
- clinmanusrawdata.xlsx